

# RINGING CHOKE CONVERTER DESIGN PROPOSAL

Igor Bertonecello Barboza  
Universidade Federal de Santa Maria  
GEDRE – Intelligence in Lighting  
Santa Maria, RS, Brazil  
igor.b.barboza@gedre.ufsm.br

Ricardo Nederson do Prado  
Universidade Federal de Santa Maria  
GEDRE – Intelligence in Lighting  
Santa Maria, RS, Brazil  
ricardo@gedre.ufsm.br

Marcelo Rafael Cosetin  
Universidade Federal de Santa Maria  
GEDRE – Intelligence in Lighting  
Santa Maria, RS, Brasil  
mcosetin@gedre.ufsm.br

**Abstract**— Nowadays regulated power sources need to be small and to have a high power density, this way they can be inserted inside small required places. These sources also should be cheaper than other circuits with the same function. This is a significant advantage, because they become more cost-effective topologies, what favors their production in large scale. This article presents the project proposal of a Ringing Choke Converter (or RCC) which can provide an average output power of 15 W. a software is used as tool to develop a project routine. After the acquisition of all RCC component values, also using tables, the simulation of this topology is done in the software LTspice. Then some simulation results are presented, including figures and values exhibition, being these compared with RCC project theory. In the sequence, the conclusions will be presented, aiming to verify if the results were achieved and to comment the contribution verified and this research continuation.

**Keywords**— Magnetism, coupling, core, saturation, BJT.

## I. INTRODUCTION

This paper aims to project a Flyback converter/RCC (Ringing Choke Converter) to feed a 15W linear load (resistor). In next works, the linear load (resistor) will be replaced by a LED lamp with a rated power of 15W.

The Ringing Choke Converter, also known as RCC, as presented in [1] e [2], is a self-oscillating Flyback converter which provides a DC output power from a DC input signal. The main characteristic of this topology (the RCC) is the core saturation, which occurs in a determined (calculated) primary winding current, ending the first operation step and beginning the second operation step. Along this paper, the circuit elements design, developed from essential electromagnetic laws, is according to Faraday's and Kirchoff's Laws.

The Section II of this paper exposes the project routine of RCC, divided in different parts, in the order the work was developed. During this section, the operation steps - including the RCC key waveforms - and other important features of the topology are approached, comprising the explanation of some design decisions and its reasons.

The Section III presents: the simulation parameters for the desired RCC operation point, according to what was obtained in the previous section; the simulation guidelines used in the used software (LTspice XVII), including the non-linearity of magnetic core; and the leading simulation results obtained.

The Section IV is the conclusion of this research, formed by the comparison between the RCC theory, the topology design proposal (showed in this paper) and the simulation results, achieved for the desired operation point.

After Section IV, the list of references follows.

## II. THE THEORY ABOUT RCC

The RCC is widely used in a lot of applications that need to present a cost-benefit relation, since it has few components and it is cheaper than other circuit elements with the same goal. According to [1], RCC is very applied in cell phone battery chargers, electronic ballasts and DC/DC converters .

This circuit received this name, according to [1], because it starts oscillating from the ringing of the transformer choke. There are many RCC topologies: using two or more saturable reactors or the saturable core activation using Zener diodes, as in [2]. However, this work aims to project the simplest Ringing Choke Converter, which configuration is exposed in Fig. 1.

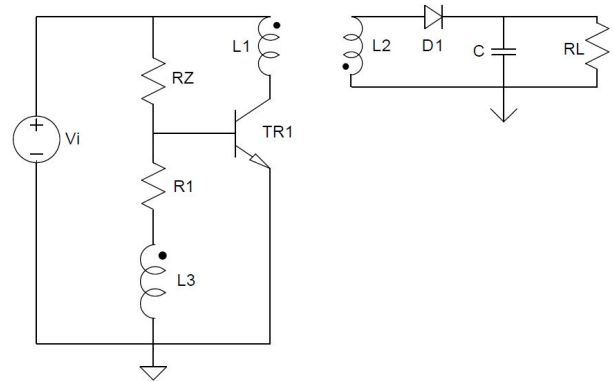


Fig. 1 – RCC Topology used in this work. From: Own authorship.

The topology elements (Fig. 1):  $V_i$  is the input voltage; TR1 is the switch; RZ and R1 are the polarization resistors; D1 is the diode, C1 the capacitor, L1 and L2 are windings; L3 is the saturable reactor (also a winding); RL is the load resistance.

### A. Input and Output Parameters Determination

According to graphics in [2], which represent the output characteristic (Current X Voltage) of a RCC for linear load, the approximated values in the operation point to provide the desired output power are: output voltage of 12V and output

current of 1.25A. With these values, the maximum output power could be, without losses, 15.6 W. Fig. 2 shows this analysis in the project routine.

In [2], the Output Current Vs RCC efficiency graphic, represented by Fig. 3, is exposed, being that this reveals that the RCC efficiency depends on the input voltage  $V_i$ . Observing Fig. 3 graphic, it was concluded that RCC presents a higher efficiency with the input voltage of 40V for the required output current (1.3A).

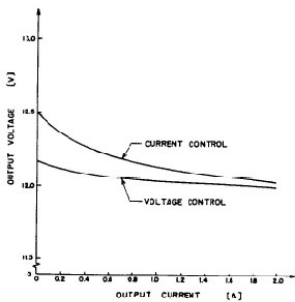


Fig. 2 - Output Current Vs Output Voltage for each control presented in the article.

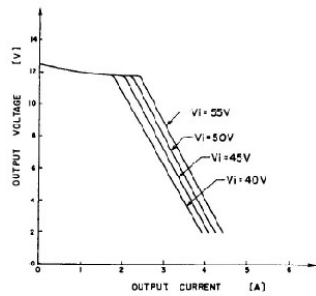


Fig. 3 - Output Current Vs Output Voltage of RCC, without any control system.

Fig. 2 – Output Characteristic Analysis, used to determinate the operation point for this application. From: [2].

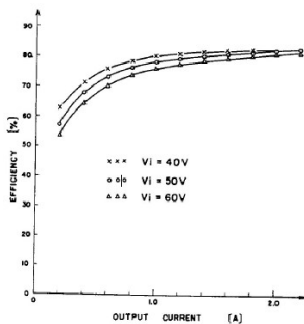


Fig. 3 – Efficiency Vs Output Current Analysis, for different  $V_i$  values. From [2]

It is possible to know the switching frequency by Fig. 4.

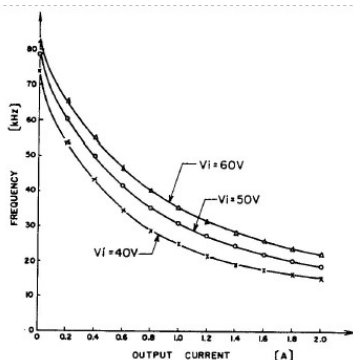


Fig. 4 – Output Current (A) Vs Switching Frequency (kHz), for different  $V_i$ . From: [2].

It was found that, for  $V_i=40V$  and  $I_{out}=1.25A$ , the switching frequency is about 20 kHz.

### RCC Operation Steps

The Ringing Choke Converter switch element is the TJB (*npn* junction) TR1, being important to mention that this topology works in three operation steps. These ones are showed in Fig. 5(a), Fig. 5(b) and Fig. 5(c).

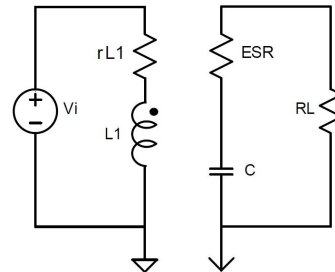


Fig. 5(a) – First operation step. From: Own authorship.

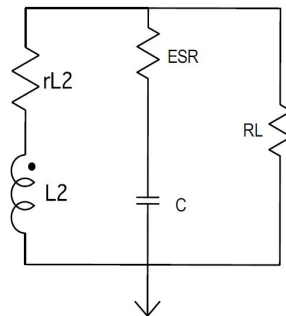


Fig. 5(b) – Second operation step. From: Own authorship.

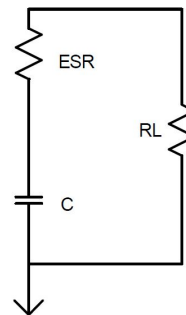


Fig. 5(c) – Third operation step. From: Own authorship.

Where:  $rL1$  is the primary winding,  $L1$ , intrinsic resistance,  $rL2$  is the secondary winding,  $L2$ , intrinsic resistance and  $ESR$  is the capacitor,  $C$ , Equivalent Series Resistance.

These three intrinsic resistances were unconsidered, for being insignificant, in the operation steps analysis that follows:

First operation step: the switch TR1 is on, the current  $I1$  passes through the winding  $L1$ , according to TR1 polarization which is being feed by the input voltage  $V_i$ , because  $V_i$  is completely applied to  $L1$ , so that the inducted voltage value in the terminals of  $L1$  is basically equal to  $V_i$ . Besides that, as this converter has coupled inductors instead of a transformer, the power transfer between the windings doesn't occur instantly; because of that, on this step, there is current passing just

through the winding L1, while the winding L2 still is not active.

The second operation step initiates when the winding L3 saturates, generating an inducted voltage in its terminals and opening the switch TR1, because this enters in the cut off region, state in which there is not collector current. Because of the magnetic coupling, an inducted voltage appears between the terminals of winding L2 and all the energy stored in L1 during the first step is now discharged by L2 in the converter output, at the same time carrying the capacitor C and providing the necessary power to the load RL.

After winding L2 has completely discharged, the winding L1 intrinsic capacitance becomes impossible to reinitiate immediately the topology operation steps, characterizing the third operation step, in which the load RL is feed just by the capacitor C, which was charged during the second step. The Figure 6 shows the key waveforms of RCC.

The Fig. 6 shows RCC operation steps, being that *Interval I* is the first operation step period of time, *Interval II* is the second and *Interval III* is the third.

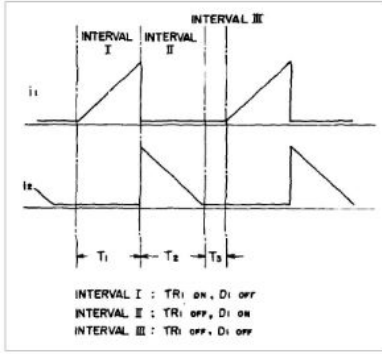


Fig. 6 – The key waveforms of the RCC topology: primary winding current  $i_1$  and secondary winding current  $i_2$ . From: [2].

### B. Coupled Inductors Project

To determinate the windings parameters, the project was done considering L1 and L2 windings inducted voltages  $V_1$  and  $V_2$  of, respectively, 40V and 12V.

It should be observed that, if there are not losses, including no diode D1 drop voltage,  $V_2$  is equal to the output voltage  $V_{out}$ . The transformation relation which makes possible to find L1 and L2 number of turns is given by (1):

$$\frac{V_1}{V_2} = \frac{N_1}{N_2} \quad (1)$$

Also the transformation relation for the winding L3 (saturable reactor) can be performed with any other winding, be L1 or be L2, since all the three windings are in the same magnetic core. (2) represents the tranformation relation between L3 and L2 (considered as primary and secondary winding, in this order).

$$\frac{V_3}{V_2} = \frac{N_3}{N_2} \quad (2)$$

It is needed to know L1 winding saturation peak current, represented as  $i_{sat}$ , because this value ensures transformer saturation. Firstly, assuming that there are not losses in this converter, the power in L1, named as  $P_1$ , and in L2, which is  $P_2$ , the power is the same, as in (3):

$$P_1 = P_2 \quad (3)$$

According to Ohm's Law, it is possible to change (3) to (4):

$$V_1 \cdot I_1 = V_2 \cdot I_2 \quad (4)$$

Mathematically manipulating (4), L1 and L2 currents, respectively,  $I_1$  and  $I_2$ , were obtained by (4) for the desired operation point:

$$I_1 = 0.375A$$

$$I_2 = 1.25A$$

Where  $I_1$  is  $i_{sat}$  itself:

$$i_{sat} = 0.375A$$

Using the Ampere's Law for this case, (5) is developed:

$$H_{sat} \cdot l_e = N_1 \cdot i_{sat} \quad (5)$$

Where  $H_{sat}$  is the magnetic field intensity saturation value, in A/m (Ampere per meter),  $l_e$  is the magnetic path average length, in m (Meter) and  $N_1$  is the number of turns of L1.

$H_{sat}$  depends on the core material characteristics, which is the reason why, at this research point, a core material had to be chosen. For being phisically available, according to [3], for presenting one of the most advantageous magnetic behaviors, the IP12E material was chosen. In the B x H curve of it, in [3], it was found, up to a temperatur of 80°C and for a frequency of 20kHz (equal to the switching frequency), the value of  $H_{sat}$  is equal to 795.775 A/m.

The next step is to choose the core. For this, the selection criteria was to get an available core produced with IP12E, an indicated material by [2]. The core also needs to have, as in [3] and [4], sufficient size to the estimated number of turns. After these observations, the chosen core was NEE 42/21/15, with the following parameters:

$$l_e = 0.097 \text{ m}$$

$$A_e = 0.000181 \text{ m}^2$$

Where  $A_e$  is the transversal section effective area, in Square meter ( $\text{m}^2$ ).

With these parameters, it is possible to calculate the number of turns of L1 winding,  $N_1$ , using (5) modified, as in (6).

$$N_1 = \frac{H_{sat} \cdot l_e}{i_{sat}} \quad (6)$$

Replacing the three right parameters by the found ones:

$$N_1 = 205.84 \text{ turns}$$

Where  $N_1$  will be approximated to 206 turns, to ensure the desired inducted voltage, based on Faraday's Law.

Aiming to find the L2 winding number of turns  $N_2$ , the parameters  $V_1$ ,  $V_2$  and  $N_1$ , already determined, are replaced in (1), where  $N_2$  is isolated to obtain:

$$N_2 = 61.752 \text{ turns}$$

Where  $N_2$  will become 62 turns to abide Faraday's Law.

Then the L3 winding number of turns,  $N_3$ , is determined. According to [2] and to observation of RCC first and second operation steps, exposed in Fig. 5(a) and Fig. 5(b), the L3 winding inducted voltage  $V_3$  should be sufficient to open the switch TR1, when L3 winding saturation occurs, in the final of the first operation step. The criteria used in this work, according to [5], is to induce a voltage  $V_3$  so that it cancels the resistor R1 voltage,  $V_{R1}$ , and leads the base-to-emitter voltage (VBE) of TR1 to zero when the saturation happens, opening the switch TR1. This way:  $V_3 = 0.82V$ .

Modifying (2),  $N_3$  was found:

$$N_3 = 4.22 \text{ turns}$$

Where  $N_3$  changes for 5 turns, for the same reason than  $N_1$  and  $N_2$ .

The wires transversal section areas, for each winding, were also determined, being used the (7), from [2]:

$$A_n = \frac{I_n}{J_s} \quad (7)$$

Where  $A_n$  is the transversal section area, in  $m^2$ ,  $I_n$  is the winding maximum effective current, in A, and  $J_s$  is the current density, in  $A/m^2$ . Briefly, being used, from [2], the general current density  $J_s$ , for inductors and transformers in Flyback converters, of:

$$J_s = 0.042 \text{ A/m}^2$$

For the three windings (L1, L2 and L3), the transversal section areas are smaller than the value of  $2,6240 \text{ mm}^2$  of AWG 13 conductor, adopted in this project, due to being the smallest existent.

Then the self and mutual inductances were calculated, in this order, (8) and (9):

$$L = \frac{\mu \cdot N^2 \cdot A_e}{D} \quad (8)$$

$$M_{ij} = \frac{\mu \cdot N_i \cdot N_j \cdot A_e}{l_e} \quad (9)$$

(10) gives the relative magnetic permeability of IP12E material, (11),  $\mu_0$ , the absolute magnetic permeability and (12),  $\mu$ , the total magnetic permeability.  $N$  is a winding number of turns,  $A_e$  is core transversal section effective area,  $D$  is winding wire total length and  $l_e$  is magnetic path effective average length, described in (13) and (14).

$$\mu_r = 5500 \quad (10)$$

$$\mu := \mu_r \mu_0 \quad (11)$$

$$\mu = 6.912 \times 10^{-3} \frac{\text{m} \cdot \text{kg}}{\text{A}^2 \cdot \text{s}^2} \quad (12)$$

$$\text{Perimeter} = 43.8 \text{mm} \quad (13)$$

$$D = N \cdot \text{Perimeter} \quad (14)$$

In which Perimeter is the sum of all transversal section area dimensions. Inductances calculations are shown in TABLE I.

TABLE I – SELF AND MUTUAL INDUCTANCES CALCULATION RESULTS

Winding	Inductances (mH)		
	L1	L2	L3
L1	5.879	163.931	11.202
L2	163.931	1.764	3.361
L3	11.202	3.361	0.121

### C. Load Determination

As mentioned in the fourth paragraph of Section II, this work starts considering a linear load, mainly because [2] also uses this load type. At this time it is necessary to calculate a load resistor  $R_L$  to accomplish with the desired operation point: output power of 15W and output voltage of 12V. Then, using an Ohm's Law modification, which is in (15), this load resistance  $R_L$  value is calculated.

$$R_L = \frac{V_{out}^2}{P_{out}} \quad (15)$$

$$R_L = 9.6 \Omega$$

### D. Capacitor Project

The capacitor  $C$  is projected analysing, basically, this RCC third operation step, seen in Fig. 5(c), because, during this step,  $R_L$  receives energy just from the capacitor. Also is needed to consider that, during the first step, capacitor  $C$  keeps being the only energy transfer element for  $R_L$ , what is also considered in this projected.

Before this analysis, it was established the switching period  $t_s$ , which is the mathematical inverse of switching frequency  $f_s$ , that is 20kHz. This way:

$$t_s = 50 \mu\text{s}$$

Each operation step period it is defined, at this point. As there were no references found which determined the duration of the operation steps and looking to become easier to visualize the simulation results behavior, the times were exposed in Fig. 7 and the periods were defined as is represented in Fig. 8.

$$t_1 := 20 \mu\text{s}$$

$$t_2 := 40 \mu\text{s}$$

$$t_3 := 50 \mu\text{s}$$

Fig. 7 – Time division to determinate operation steps duration. From: Own authorship.

$$\text{1st Operation Step} \quad t_1 = 20 \mu\text{s}$$

$$\text{2nd Operation Step} \quad t_2 - t_1 = 20 \mu\text{s}$$

$$\text{3rd Operation Step} \quad t_3 - t_2 = 10 \mu\text{s}$$

Fig. 8 – Operation steps periods. From: Own authorship.

The voltage equation for capacitors is used, given by (16).

$$VC = V_0 + \frac{1}{C} \int iC(t) dt \quad (16)$$

Where:  $VC$  is the capacitor voltage, in Volts (V),  $V_0$  is the initial capacitor voltage, in Volts (V),  $C$  is the capacitance, in Farad (F),  $iC$  is the capacitor current, in Ampere (A), and  $t$  is the time, in Seconds (s).

Considering  $V_0$  equals to 0V and ignoring the capacitors ESR (Equivalent Series Resistance), the Kirchhoff's Laws were applied to this case and, after equations development, to calculate the capacitance  $C$ , (17) was obtained.

$$C = \frac{iC}{VRL} \int_{t_2}^{t_3} 1 dt \quad (17)$$

Applying the Ohm's Law in the closed loop of third operation step, it gives origin to (18). Solving (17) and then replacing (18) in (17), (19) is obtained.

$$\frac{1}{RL} = \frac{iC}{VRL} \quad (18)$$

$$C = \frac{t_3 - t_2}{RL} \quad (19)$$

However (19) shows just the third operation step period, the first one has to be included, as follows in (20).

$$C = \frac{etapa3 + t1}{RL} \quad (20)$$

Replacing the calculated values in (20), where  $etapa3$  is equal to 3<sup>rd</sup> Operation Step, it was found the capacitor value  $C$ .

$$C = 3.125 \mu F$$

### E. Polarization Circuit Project

It is based in the first operation step, because this circuit aims to bias the switch TR1 in the desired operation point. In *Item B*, the current  $I_1$ , which passes in the winding L1 (equal to collector current  $IC$  of TR1) was determined. Fig. 10 expresses this relation:

$$\begin{aligned} isat &= IC = I_1 \\ IC &= 0.375 A \end{aligned}$$

Fig. 10 – Current values in the first operation step. From: Own authorship.

It is essential to choose a power BJT as TR1. The selection criteria was to find an available power BJT which could stand the necessary collector current. BC337-40, a silicon *npn* junction BJT was selected.

The polarization circuit is formed by the resistores  $R1$  and  $RZ$ . [4] suggests a total resistance value ( $Rtotal$ ), which is shown by (23).

$$Rtotal = R1 + RZ \quad (23)$$

The Kirchhoff's Laws were applied in  $V_i$  closed loop, that can be seen in Fig. 1, being that this development ends in a

second degree polynomial equation, solved through Bhaskara's method, with the positive and negative results, respectively, represented by (24) and (25).

$$R1_{pos} = \frac{\left(\frac{-V_i}{IB} + Rtotal\right) + \sqrt{\left(\frac{V_i}{IB} - Rtotal\right)^2 + 4 \cdot r_{\pi} \cdot Rtotal}}{2} \quad (24)$$

$$R1_{neg} = \frac{\left(\frac{-V_i}{IB} + Rtotal\right) - \sqrt{\left(\frac{V_i}{IB} - Rtotal\right)^2 + 4 \cdot r_{\pi} \cdot Rtotal}}{2} \quad (25)$$

Where:  $IB$  is base current,  $V_i$  is input voltage,  $Rtotal$  is the total polarization circuit resistance and  $r_{\pi}$  is the dynamic intrinsic base-emitter resistance.

By BC337-40 datasheet and its simulation, as a current source, the desired operation point ( $IC = 0.375 A$ ) occurs when the base-to-emitter voltage  $V_{BE}$  is around 0.82V. This means that the voltage  $VR1$  (in resistor  $R1$ ) is 0.82V. The experimental current gain  $\beta$ , for the operation point, is around 426. Then the base current  $IB$  was found, as follows in Fig. 11.

$$\begin{aligned} IC &= 0.375 A \\ \beta &= 426 \\ IB &= \frac{IC}{\beta} \\ IB &= 880.282 \mu A \end{aligned}$$

Fig. 11 – Base current calculation. From: Own authorship.

With  $IB$  value, it is possible to calculate  $r_{\pi}$ , using (26):

$$r_{\pi} = \frac{V_{BE}}{IB} \quad (26)$$

Replacing the found values in (26):

$$r_{\pi} = 931.52 \Omega$$

(27) describes an other important suggested criteria, also from [4], which is applied to this case:

$$Rtotal = 100 \cdot r_{\pi} \quad (27)$$

$$Rtotal = 93.152 k\Omega$$

Replacing  $V_i$ ,  $IB$ ,  $Rtotal$  and  $r_{\pi}$  in (24) and in (25), respectively, two resistance results are obtained, however just the positive one is used, so that  $R1_{pos}$  was selected:

$$R1 = R1_{pos} = 49.466 k\Omega$$

Using  $R1$  value in (23) and isolating  $RZ$  in it, it is found:

$$RZ = 43.686 k\Omega$$

### III. RCC SIMULATION

The RCC simulation was done in LTspice. In Fig. 12, there is the complete schematic of the designed RCC simulation.



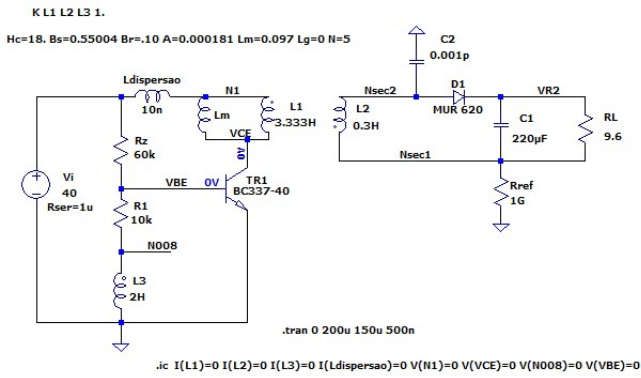


Fig. 12 – Complete RCC simulation schematic. From: Own authorship.

It was observed that the capacitor value was not sufficient to keep the load feed during the third operation step, so it was adjusted to the desired output voltage value (12V). The elements *Ldispersao* and *Lm* represent, respectively, core dispersion inductance and core magnetizing inductance, being that these, mainly the last one, are the core non-linear features needed to guarantee its saturation [5] [6]. Fig. 13 to 16 shows main simulation results waveforms.

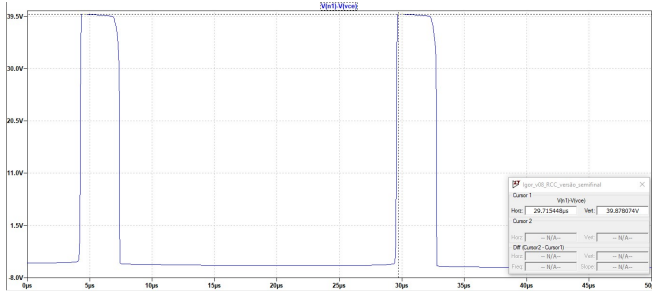


Fig. 13 – The waveform (in blue) of simulation result for the winding N1 induced voltage: 39.87V. From: LTSpice.

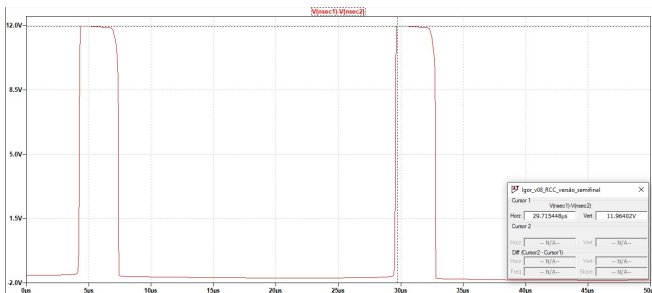


Fig. 14 – The waveform (in red) of simulation result for the winding N2 induced voltage: 11.96V. From: LTSpice.

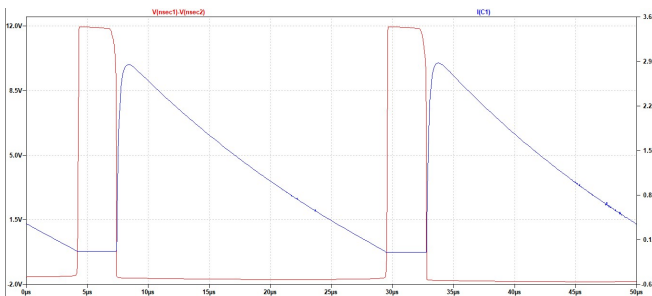


Fig. 15 – Waveforms for simulation results of N1 current (or collector current IC, in red) and induced voltage (in blue). When core saturates, TR1 switch goes off and there is not N1 induced voltage. From: LTSpice.

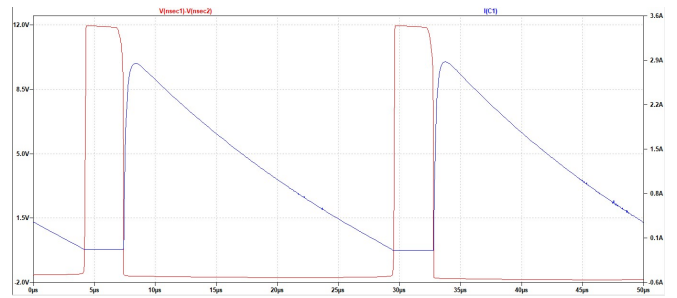


Fig. 16 - Waveforms for simulation results of winding N2 induced voltage (in red) compared to the C1 capacitor current (in blue). From: LTSpice.

#### IV. CONCLUSION

After this work, it is observed that, however C1 capacitor and L3 winding projects were not totally right, after these and other modifications, as core non-linear features in simulation guidelines, following the other parts of this design proposal, the RCC typical waveforms were verified and the load keeps always feed, according to the expected, since output voltage, in Fig.14, reaches the desired value (close to 12V) during a period of time and, in the rest of commutation period of time, the capacitor C perfectly maintain the output voltage (as can be seen in Fig.16).

#### REFERENCES

- [1] T. K. Hareendran, from ELECTRO SCHEMATICS. “DIY RCC SMPS Circuits”. Internet: <https://www.electroschematics.com/12799/diy-rcc-smps-circuits/>, July 2016 [July 05, 2018].
- [2] M. Kohno and E. Miyachika. “A Saturable Reactor Controlled Ringing Choke Converter”, in *INTELEC – 1979 International Telecommunications Energy Conference*, 26-29 Nov. 1979, pp. 1-7.
- [3] THORNTON ELETRÔNICA LTDA. “Material – IP12E”. Internet: [http://www.thornton.com.br/materiais\\_ip12e\\_ing.htm](http://www.thornton.com.br/materiais_ip12e_ing.htm), April 2008 [June 20, 2018].
- [4] RAZAVI, Behzad. "Fundamentals of Microelectronics". 1ª edição. LTC Editor, 2010.
- [5] Shi Ping Hsu. “TRANSFORMER MODELING AND DESIGN FOR LEAKAGE CONTROL”. *R.D. Middlebrook and Slobodan Cuk, Power Conversion International*, pg. 68, Feb. 1982.
- [6] L. G. Meares and Charles E. Hymowitz. “SPICE Models For Power Electronics”. Internet: <http://www.intusoft.com/articles/satcore.pdf>, May 2012 [July 11, 2018].